6th International Conference on Applied Informatics
Eger, Hungary, January 27–31, 2004.

On Spatial Involute Gearing

Hellmuth Stachel

Institute of Discrete Mathematics and Geometry, Vienna University of Technology
e-mail: stachel@dmg.tuwien.ac.at

Abstract

This is a geometric approach to spatial involute gearing which has recently been developed by Jack Phillips [2]. New proofs of Phillips' fundamental theorems are given. And it is pointed out that also a permanent straight line contact is possible for conjugate helical involutes. In addition, the gearing is illustrated in various ways.

Key Words and Phrases: Spatial gearing, involute gearing, helical involute

1 Basic kinematics of the gear set

The function of a gear set is to transmit a rotary motion of the input wheel Σ_1 about the axis p_{10} with angular velocity ω_{10} to the output wheel Σ_2 rotating about p_{20} with ω_{20} in a uniform way, i.e., with a constant *transmission ratio*

$$i := \omega_{20}/\omega_{10} = \text{const.} \tag{1}$$

According to the relative position of the gear axes p_{10} and p_{20} we distinguish the following types (see Fig. 1):

a) Planar gearing (*spur gears*) for parallel axes p_{10}, p_{20},
b) spherical gearing (*bevel gears*) for intersecting axes p_{10}, p_{20}, and
c) spatial gearing (*hyperboloidal gears*) for skew axes p_{10}, p_{20}, in particular *worm gears* for orthogonal p_{10}, p_{20}.

1.1 Planar gearing

In the case of parallel axes p_{10}, p_{20} we confine us to a perpendicular plane where two systems Σ_1, Σ_2 are rotating against Σ_0 about centers 10, 20 with velocities ω_{10}, ω_{20}, respectively. Two curves $c_1 \subset \Sigma_1$ and $c_2 \subset \Sigma_2$ are *conjugate* profiles when they are in permanent contact during the transmission, i.e., (c_2, c_1) is a pair of enveloping curves under the relative motion Σ_2/Σ_1. Due to a standard theorem from plane kinematics (see, e.g., [5] or [1]) the common normal at the point E of contact must pass through the pole 12 of this relative motion. The planar Three-Pole-Theorem states that 12 divides the segment 01 02 at the constant ratio i. Hence also 12 is fixed in Σ_0. We summarize:

a) *spur gears* b) *bevel gears* c) *hyperboloidal gears* e.g. *worm gears*

Figure 1: Types of gears

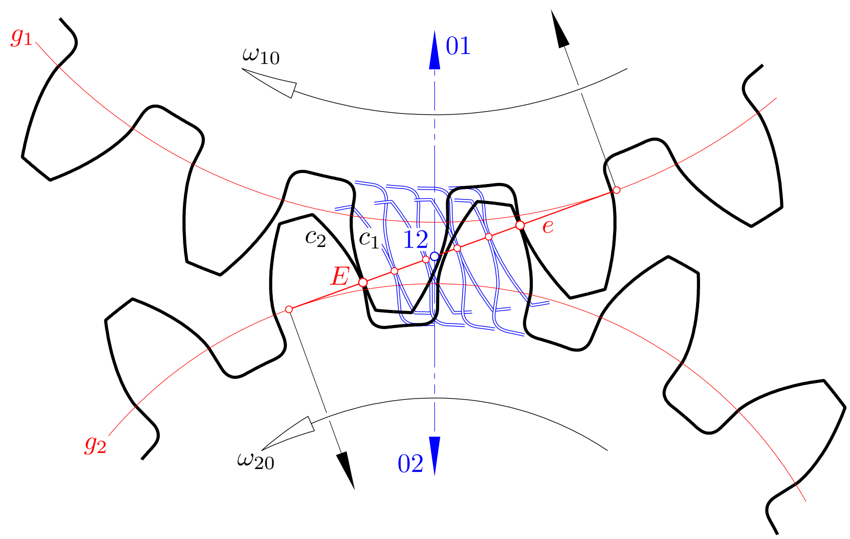

Figure 2: Planar involute gearing

Theorem 1.1 (Fundamental law of planar gearing):
The profiles $c_1 \subset \Sigma_1$ and $c_2 \subset \Sigma_2$ are conjugate if and only if the common normal e (=meshing normal) at the point E of contact (=meshing point) passes through the relative pole 12.

Due to L. Euler (1765) planar *involute gearing* (see Fig. 2) is characterized by the condition that with respect to the fixed system Σ_0 *all meshing normals e are coincident.* This implies

(i) The profiles are involutes of the base circles, i.e., circles tangent to the meshing normal and centered at 01, 02, respectively.

(ii) For constant driving velocity ω_{10} the point of contact E runs relative to Σ_0 with constant velocity along e.

(iii) The transmitting force has a fixed line of action.

(iv) The transmission ratio depends only on the dimensions of the curves c_1, c_2 and not on their relative position. Therefore this planar gearing remains *independent of errors upon assembly.*

1.2 Basics of spatial kinematics

There is a tight connection between spatial kinematics and the geometry of lines in the Euclidean 3-space $\mathbb{E}^3$.

1.2.1 Metric line geometry in $\mathbb{E}^3$

Any oriented line (*spear*) $g = \mathbf{a} + \mathbb{R}\mathbf{g}$ can be uniquely represented by the pair of vectors $(\mathbf{g}, \widehat{\mathbf{g}})$, the *direction vector* $\mathbf{g}$ and the *momentum vector* $\widehat{\mathbf{g}}$, with

$$\mathbf{g}.\mathbf{g} = 1 \quad \text{and} \quad \widehat{\mathbf{g}} := \mathbf{a}\times\mathbf{g}.$$

It is convenient to combine this pair to a *dual vector*

$$\underline{\mathbf{g}} := \mathbf{g} + \varepsilon\widehat{\mathbf{g}},$$

where the dual unit ε obeys the rule $\varepsilon^2 = 0$. We extend the usual dot product of vectors to dual vectors and notice

$$\underline{\mathbf{g}} \cdot \underline{\mathbf{g}} = \mathbf{g}.\mathbf{g} + 2\mathbf{g}.\widehat{\mathbf{g}} = 1 + \varepsilon\, 0 = 1\,.$$

Hence we call $\underline{\mathbf{g}}$ a *dual unit vector.*

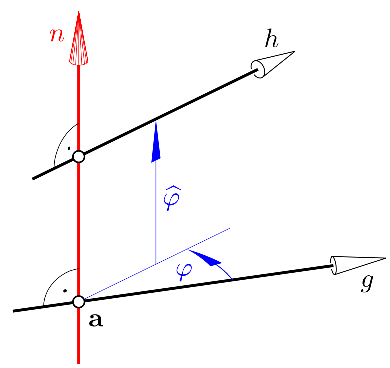

Figure 3: Two spears g, h with the dual angle $\underline{\varphi} = \varphi + \varepsilon\widehat{\varphi}$

Theorem 1.2 *There is a bijection between oriented lines (spears) g in $\mathbb{E}^3$ and dual unit vectors $\underline{\mathbf{g}}$*

$$g \;\mapsto\; \underline{\mathbf{g}} = \mathbf{g} + \varepsilon\widehat{\mathbf{g}} \quad \textit{with} \quad \underline{\mathbf{g}} \cdot \underline{\mathbf{g}} = 1\,.$$

The following theorem reveals the geometric meaning of the dot product and the cross product of dual unit vectors, expressed in terms of the *dual angle* (see Fig. 3) $\underline{\varphi} = \varphi + \varepsilon\widehat{\varphi}$ between g und h, i.e., with $\varphi = \sphericalangle gh$ and $\widehat{\varphi}$ as shortest distance between the straight lines (compare [3], p. 155 ff):

Theorem 1.3 *Let $\underline{\varphi} = \varphi + \varepsilon\widehat{\varphi}$ be the dual angle between the spears g and h and let n be a spear along a common perpendicular. Then we have*

$$\begin{aligned} \cos\varphi - \varepsilon\widehat{\varphi}\sin\varphi &= \underline{\cos\varphi} = \underline{\mathbf{g}}\cdot\underline{\mathbf{h}} = \mathbf{g}.\mathbf{h} + \varepsilon(\widehat{\mathbf{g}}.\mathbf{h} + \mathbf{g}.\widehat{\mathbf{h}}),\\ (\sin\varphi + \varepsilon\widehat{\varphi}\cos\varphi)(\mathbf{n} + \varepsilon\widehat{\mathbf{n}}) &= \underline{\sin\varphi}\,\underline{\mathbf{n}} = \underline{\mathbf{g}}\times\underline{\mathbf{h}} = \mathbf{g}\times\mathbf{h} + \varepsilon(\widehat{\mathbf{g}}\times\mathbf{h} + \mathbf{g}\times\widehat{\mathbf{h}}). \end{aligned}$$

The components $\varphi, \widehat{\varphi}$ of the dual angle $\underline{\varphi}$ are signed according to the orientation of the common perpendicular n. When the orientation of n is reversed then φ and $\widehat{\varphi}$ change their sign. When the orientation either of g or of h is reversed then φ has to be replaced by $\varphi + \pi \pmod{2\pi}$. Hence, the product $(\widehat{\varphi}\tan\varphi)$ is invariant against any change of orientation.

$\underline{\mathbf{g}} \cdot \underline{\mathbf{h}} = 0$ characterizes perpendicular intersection.

1.2.2 Instantaneous screw

There is also a geometric interpretation for dual vectors which are not unit vectors: At any moment a spatial motion Σ_i/Σ_j assigns to the point $X \in \Sigma_i$ (coordinate vector $\mathbf{x}$) the *velocity vector*

$$ {}_X\mathbf{v}_{ij} = \widehat{\mathbf{q}}_{ij} + (\mathbf{q}_{ij} \times \mathbf{x}). \tag{2} $$

relative to Σ_j. We combine the pair $(\mathbf{q}_{ij}, \widehat{\mathbf{q}}_{ij})$ again to a dual vector $\underline{\mathbf{q}}_{ij}$. This vector can always be expressed as a multiple of a unit vector, i.e.,

$$ \underline{\mathbf{q}}_{ij} := \mathbf{q}_{ij} + \varepsilon \widehat{\mathbf{q}}_{ij} = (\omega_{ij} + \varepsilon\, \widehat{\omega}_{ij})(\mathbf{p}_{ij} + \varepsilon\, \widehat{\mathbf{p}}_{ij}) = \underline{\omega}_{ij}\, \underline{\mathbf{p}}_{ij} \quad \text{with} \quad \underline{\mathbf{p}}_{ij} \cdot \underline{\mathbf{p}}_{ij} = 1\,. \tag{3} $$

It turns out that ${}_X\mathbf{v}_{ij}$ coincides with the velocity vector of X under a helical motion (= *instantaneous screw motion*) about the *instantaneous axis* p_{ij} with dual unit vector $\underline{\mathbf{p}}_{ij}$. The dual factor $\underline{\omega}_{ij}$ is a compound of the angular velocity ω_{ij} and the translatory velocity $\widehat{\omega}_{ij}$ of this helical motion. $\underline{\mathbf{q}}_{ij}$ is called the *instantaneous screw*.

For each instantaneous motion (screw $\underline{\mathbf{q}}_{ij}$) the *path normals* n constitute a *linear line complex*, the (= *complex of normals*) as the dual unit vector $\underline{\mathbf{n}} = \mathbf{n} + \varepsilon \widehat{\mathbf{n}}$ of any normal n obeys the equation

$$ \widehat{\mathbf{q}}_{ij}.\mathbf{n} + \mathbf{q}_{ij}.\widehat{\mathbf{n}} = 0 \quad (\Longleftrightarrow\ \underline{\mathbf{q}}_{ij} \cdot \underline{\mathbf{n}} \in \mathbb{R}). \tag{4} $$

This results from ${}_X\mathbf{v}_{ij}.\mathbf{n} = 0$ and $\widehat{\mathbf{n}} = \mathbf{x} \times \mathbf{n}$. By Theorem 1.3 it is equivalent to

$$ (\omega_{ij} + \varepsilon\widehat{\omega}_{ij})\, \underline{\cos\alpha} \in \mathbb{R} \quad \text{or} \quad \widehat{\omega}_{ij}/\omega_{ij} = \widehat{\alpha}\, \tan\alpha \tag{5} $$

with $\underline{\alpha}$ as dual angle between p_{ij} and any orientation of n.

The following is a standard result of spatial kinematics (see e.g. [1] or [4]):

Theorem 1.4 (Spatial Three-Pole-Theorem):
If for three given systems $\Sigma_0, \Sigma_1, \Sigma_2$ the dual vectors $\underline{\mathbf{q}}_{10}$, $\underline{\mathbf{q}}_{20}$ are the instantaneous screws of Σ_1/Σ_0, Σ_2/Σ_0, resp., then

$$ \underline{\mathbf{q}}_{21} = \underline{\mathbf{q}}_{20} - \underline{\mathbf{q}}_{10} $$

is the instantaneous screw of the relative motion Σ_2/Σ_1.

Let the line n (dual unit vector $\underline{\mathbf{n}}$) orthogonally intersect both axes $\underline{\mathbf{p}}_{10}$ of Σ_1/Σ_0 and $\underline{\mathbf{p}}_{20}$ of Σ_2/Σ_0. Then n does the same with the axis $\underline{\mathbf{p}}_{21}$ of Σ_2/Σ_1, provided $\omega_{21} \neq 0$. This follows from

$$ \underline{\mathbf{n}} \cdot \underline{\mathbf{p}}_{10} = \underline{\mathbf{n}} \cdot \underline{\mathbf{p}}_{20} = 0 \implies \underline{\omega}_{21}(\underline{\mathbf{n}} \cdot \underline{\mathbf{p}}_{21}) = \underline{\omega}_{20}(\underline{\mathbf{n}} \cdot \underline{\mathbf{p}}_{20}) - \underline{\omega}_{10}(\underline{\mathbf{n}} \cdot \underline{\mathbf{p}}_{10}) = 0, $$

and there exists an inverse $\underline{\omega}_{21}^{-1}$.

1.2.3 Fundamentals of spatial gearing

Let the systems Σ_1, Σ_2 rotate against Σ_0 about the fixed axes p_{10}, p_{20} with constant angular velocities ω_{10}, ω_{20}, respectively. Then the instantaneous screw of the relative motion Σ_2/Σ_1 is constant in Σ_0, too. It reads

$$ \underline{\mathbf{q}}_{21} = \omega_{20}\, \underline{\mathbf{p}}_{20} - \omega_{10}\, \underline{\mathbf{p}}_{10} \quad \text{for} \quad \omega_{10}, \omega_{20} \in \mathbb{R}\,. \tag{6} $$

When two surfaces $\Phi_1 \subset \Sigma_1$ and $\Phi_2 \subset \Sigma_2$ are *conjugate* tooth flanks for a uniform transmission, then Φ_1 contacts Φ_2 permanently under the relative motion Σ_2/Σ_1. In analogy to the planar case (Theorem 1.1) we obtain

Theorem 1.5 (Fundamental law of spatial gearing):
The tooth flanks $\Phi_1 \in \Sigma_1$ and $\Phi_2 \in \Sigma_2$ are conjugate if and only if at each point E of contact (=meshing point) the contact normal (=meshing normal) e is included in the complex of normals of the relative motion Σ_2/Σ_1.

Due to (4) the dual unit vector $\underline{\mathbf{e}}$ of any meshing normal e obeys the equation of the linear line complex

$$\underline{\mathbf{q}}_{21} \cdot \underline{\mathbf{e}} = \omega_{20} \, (\underline{\mathbf{p}}_{20} \cdot \underline{\mathbf{e}}) - \omega_{10} \, (\underline{\mathbf{p}}_{10} \cdot \underline{\mathbf{e}}) \in \mathbb{R}.$$

Hence Theorem 1.3 implies for the dual angles $\underline{\alpha}_1$, $\underline{\alpha}_2$ between e and p_{10} and p_{20}, resp., (see Fig. 3, compare [2], Fig. 2.02, p. 46)

$$\omega_{20}\widehat{\alpha}_2 \sin\alpha_2 - \omega_{10}\widehat{\alpha}_1 \sin\alpha_1 = 0 \quad\Longrightarrow\quad i = \frac{\omega_{20}}{\omega_{10}} = \frac{\widehat{\alpha}_1 \sin\alpha_1}{\widehat{\alpha}_2 \sin\alpha_2}\,. \tag{7}$$

2 J. Phillips' spatial involute gearing

In [2] Jack Phillips characterizes the spatial involute gearing in analogy to the planar case as follows: This is a gearing with point contact where *all meshing normals e are coincident in Σ_0 — and skew to p_{10} and p_{20}*. We exclude also perpendicularity between e and one of the axes. According to (7) this meshing normal e determines already a constant transmission ratio.

In the next section we determine possible tooth flanks Φ_1, Φ_2 for such an involute gearing. At any point E of contact the common tangent plane ε of Φ_1, Φ_2 is *orthogonal to e*.

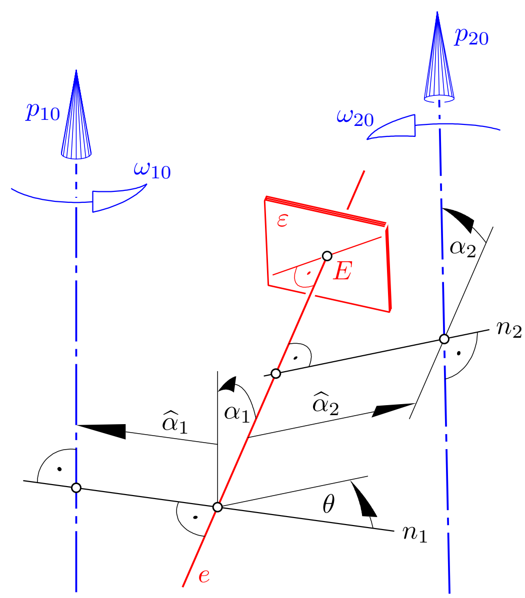

Figure 4: Spatial involute gearing with the meshing point E tracing the fixed meshing normal e

2.1 Slip tracks

First we focus on the paths of the meshing point E relative to the wheels Σ_1, Σ_2. These paths are called *slip tracks* c_1, c_2:

2.1.1 Slip tracks as orthogonal trajectories

Σ_1/Σ_0 is a rotation about p_{10}, and we have $E \in e$ where e is fixed in Σ_0. Therefore this slip track c_1 is located on the *one-sheet hyperboloid* Π_1 *of revolution* through e with axis p_{10}.

The point of contact E is located on Φ_1; therefore the line tangent to the slip track c_1 is orthogonal to e. This leads to our fist result:

Lemma 2.1 *The path c_1 of E relative to Σ_1 is an orthogonal trajectory of the e-regulus on the one-sheet hyperboloid Π_1 through e with axis p_{10}.*

Let this hyperboloid $\Pi_1 \subset \Sigma_1$ with point E rotate about p_{10} with the constant angular velocity ω_{10}, while simultaneously E runs relative to Σ_1 along c_1 (velocity vector ${}_E\mathbf{v}_1$) such that E traces in Σ_0 the fixed meshing normal e (velocity vector ${}_E\mathbf{v}_0$). For the sake of brevity we call this movement the *"absolute motion" of E via* Σ_1. The velocity vector of E under this absolute motion is

$$ {}_E\mathbf{v}_0 = {}_E\mathbf{v}_1 + {}_E\mathbf{v}_{10} \tag{8} $$

with ${}_E\mathbf{v}_{10}$ stemming from the rotation Σ_1/Σ_0 about p_{10}.

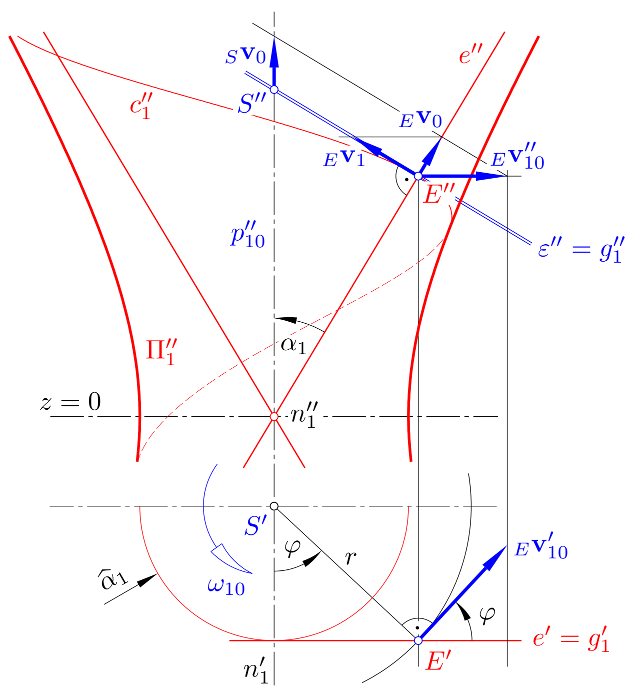

Figure 5: The velocities of the meshing point E relative to Σ_1 and Σ_0

We check the front view in Fig. 5 with p_{10} and e being parallel to the image plane. Hence the tangent plane $\varepsilon \perp e$ is displayed as a line.

Let r denote the instantaneous distance of E from p_{10}. Then we have $\|_E\mathbf{v}_{10}\| = r\omega_{10}$. In the front view of Fig. 5 we see the length

$$\|_E\mathbf{v}''_{10}\| = |r\omega_{10}\cos\varphi| = |\widehat{\alpha}_1\omega_{10}| = \text{const.}$$

with $\widehat{\alpha}_1$ as the shortest distance between e and p_{10} — as used in (7) and Fig. 4. This implies a constant velocity of E also against Σ_0 along e, namely

$$\|_E\mathbf{v}_0\| = |\widehat{\alpha}_1\omega_{10}\sin\alpha_1| = \text{const.} \quad \text{with} \quad \alpha_1 = \sphericalangle\, e\, p_{10}. \tag{9}$$

When E moves with constant velocity along e, then the point S of intersection between the plane ε of contact ($\varepsilon \perp e$) and p_{10} moves with constant velocity, too. We get

$$\|_S\mathbf{v}_0\| = |\widehat{\alpha}_1\omega_{10}\tan\alpha_1| = \text{const.} \tag{10}$$

This means, that ε performs relative to Σ_1 a rotation about p_{10} with constant angular velocity $-\omega_{10}$ and a translation along p_{10} with constant velocity $\|_S\mathbf{v}_0\|$. So, the envelope Φ_1 of ε in Σ_1 is a *helical involute* (= developable helical surface), formed by the tangent lines g_1 of a helix (see Fig. 7) with axis p_{10}, with radius $\widehat{\alpha}_1$ and with pitch $\widehat{\alpha}_1\tan\alpha_1$.[1]

Lemma 2.2 *The slip track c_1 is located on a helical involute Φ_1 with the pitch $\widehat{\alpha}_1\tan\alpha_1$. At each point $E \in c_1$ there is an orthogonal intersection between Φ_1 and the one-sheet hyperboloid Π_1 mentioned in Lemma 2.1.*

We resolve equation (8) for the vector $_E\mathbf{v}_1$, which is tangent to the slip track $c_1 \subset \Phi_1$, and obtain

Corollary 2.3 *The velocity vector $_E\mathbf{v}_1$ of the slip track c_1 at any point E is the image of the negative velocity vector $-_E\mathbf{v}_{10}$ of the rotation Σ_1/Σ_0 under orthogonal projection into the tangent plane ε of Φ_1.*

2.1.2 The tooth flanks

The simplest tooth flank for point contact is the envelope Φ_1 of the plane ε of contact in Σ_1. Hence we can summarize:

Theorem 2.1 (Phillips' 1st Fundamental Theorem:)
The helical involutes Φ_1, Φ_2 are conjugate tooth flanks with point contact for a spatial gearing where all meshing normals coincide with a line e fixed in Σ_0.

Fig. 5 shows one generator g_1 of the helical involute Φ_1. At E there is a triad of three mutually perpendicular lines, the generator g_1 of Φ_1, the generator e of the hyperboloid Π_1, and the line which is parallel to the common normal n_1 of e and p_1.

The screw motion about the axis p_{10} which generates the helical involute Φ_1 has also a linear complex of normals. The e-regulus of the one-sheet hyperboloid Π_1 is subset of this complex. Thus, with eq. (5) we can confirm the pitch of Φ_1 as stated in Lemma 2.2.

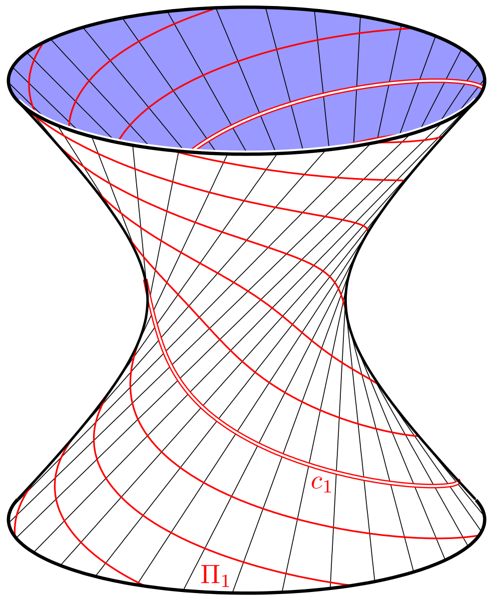

Figure 6: Slip tracks c_1 as orthogonal trajectories on the one-sheet hyperboloid Π_1

2.1.3 The continuum of slip tracks on Π_1 and on Φ_1

In Figures 6 and 7 different slip tracks c_1 are displayed, either on the one-sheet hyperboloid Π_1 or on the helical involute Φ_1.

Let p_{10} be the z-axis of a cartesian coordinate system with the plane $z = 0$ containing the throat circle of Π_1 (see Fig. 5). Then the slip track c_1 which starts in the plane $z = 0$ on the x-axis can be parametrized as

$$c_1(t)\colon \begin{pmatrix} x(t) \\ y(t) \\ z(t) \end{pmatrix} = \widehat{\alpha}_1 \begin{pmatrix} \cos t \\ \sin t \\ 0 \end{pmatrix} + \widehat{\alpha}_1 t \sin\alpha_1 \begin{pmatrix} \sin\alpha_1 \sin t \\ -\sin\alpha_1 \cos t \\ \cos\alpha_1 \end{pmatrix}. \tag{11}$$

This follows from (9) or from the differential equation expressing the perpendicularity between c_1 and the e-regulus. The different slip tracks on Π_1 arise from each other by rotation about p_{10}.

The same curve can also be written as

$$c_1(t)\colon \begin{pmatrix} x(t) \\ y(t) \\ z(t) \end{pmatrix} = \widehat{\alpha}_1 \begin{pmatrix} \cos t \\ \sin t \\ t\tan\alpha_1 \end{pmatrix} - \widehat{\alpha}_1 t \sin^2\alpha_1 \begin{pmatrix} -\sin t \\ \cos t \\ \tan\alpha_1 \end{pmatrix}. \tag{12}$$

This shows c_1 as a curve on the helical involute Φ_1 as

1. the first term on the right hand side parametrizes the edge of regression of Φ_1;
2. the second term has the direction of generators $g_1 \subset \Phi_1$.

[1] The signed distances $\alpha_1, \widehat{\alpha}_1$ specified in Figures 5 und 6 give $\widehat{\alpha}_1 \tan\alpha_1 < 0$. In Fig. 7 the pitch of Φ_1 is positive.

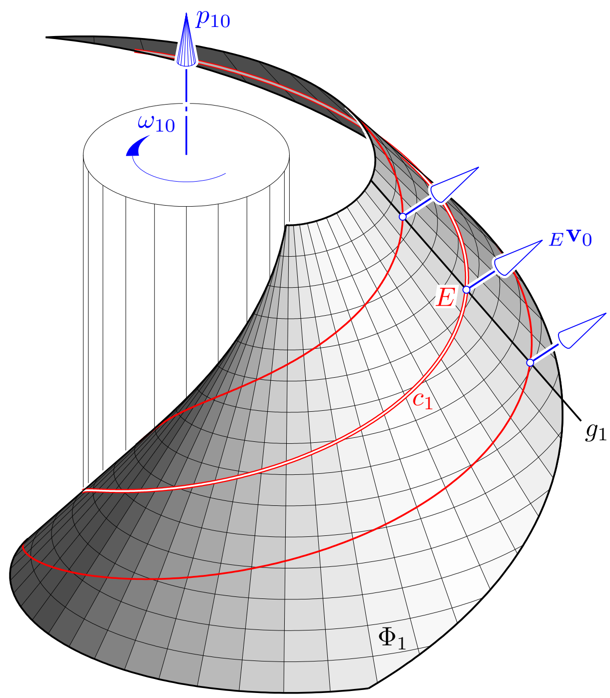

Figure 7: The tooth flank Φ_1 (helical involute) with the slip track c_1 of point $E \in g_1$

The lengths along g_1 is proportional to the angle t of rotation measured from the starting point. Therefore any two different slip tracks on Φ_1 (see Fig. 7) enclose on each generator a segment of the same length.

The different slip tracks on Φ_1 arise from each other by helical motions about p_{10} with pitch $\widehat{\alpha}_1 \tan\alpha_1$ according to Lemma 2.2. The slip tracks c_1 on Φ_1 are characterized by the following property: If a rotation of Φ_1 about its axis p_1 is combined with a movement of point E on Φ_1 such that this point E traces relative to Σ_0 a surface normal e of Φ_1, then the path $c_1 \subset \Phi_1$ of E on Φ_1 must be a slip track.

In the sense of Corollary 2.3 the slip tracks are the *integral curves* of the vector field of Φ_1 which consists of the tangent components of the velocity vectors under the rotation Σ_1/Σ_0.

2.2 Two helical involutes in contact

Theorem 2.2 (Phillips' 2nd Fundamental Theorem:)
If two given helical involutes Φ_1, Φ_2 are placed in mutual contact at point E and if their axes are kept fixed in this position, then Φ_1 and Φ_2 serve as tooth flanks for uniform transmission whether the axes are parallel, intersecting or skew.
According to (7) the transmission ratio i depends only on Φ_1 and Φ_2 and not on their relative position. Therefore this spatial gearing remains independent of errors upon assembly.

Proof: When Φ_1 rotates with constant angular velocity about the axis p_{10} and point E

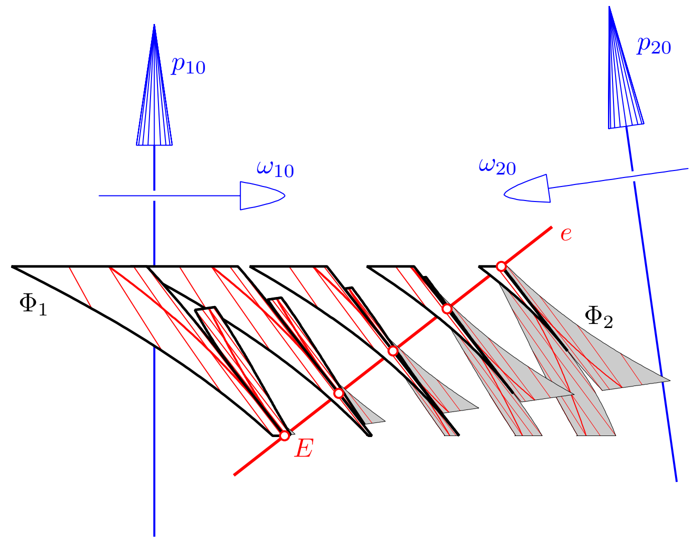

Figure 8: Different postures of Φ_1 and Φ_2 with line contact

runs relative to Φ_1 along the slip track with ${}_E\mathbf{v}_1$ according to (8), then E traces in Σ_0 a line e which remains normal to Φ_1. By (9) the velocity of E under this absolute motion is $\|{}_E\mathbf{v}_0\| = |\widehat{\alpha}_1\omega_{10}\sin\alpha_1|$.

Due to (7) E gets the same velocity vector along e under the analogous absolute motion via Σ_2. Hence the contact between Φ_1 and Φ_2 at E is preserved under the simultaneous rotations with transmission ratio i from (7). □

This means that the advantages (ii)–(iv) of planar involute gearing as listed above are still true for spatial involute gearing.

The velocity vector ${}_E\mathbf{v}_0$ of the absolute motions via Σ_1 or Σ_2 does not change when E varies on the generators $g_1 \subset \Phi_1$ (see Fig. 7)[2] or on $g_2 \subset \Phi_2$. Hence both generators perform a translation in direction of e under the absolute motions of their points via Σ_1 or Σ_2.

It has already been pointed out that $g_i \subset \varepsilon$, $i = 1, 2$, is perpendicular to the common normal n_i between p_{i0} and e (note Fig. 5). Hence the angle between g_1 and g_2 is congruent to the angle θ between n_1 and n_2 (see Fig. 4). This proves

Theorem 2.3 *Under the uniform transmission induced by two contacting helical involutes Φ_1, Φ_2 according to Theorem 2.2 the angle θ between the generators $g_1 \subset \Phi_1$ and $g_2 \subset \Phi_2$ at the point E of contact remains constant (see Fig. 10).*
This angle is congruent to the angle made by the common normals n_1, n_2 between e and the axes p_{10}, p_{20}.

[2]Note that all normal lines of the helical involute Φ_1 make the same dual angle $\alpha_1 + \varepsilon\widehat{\alpha}_1$ with the axis p_{10}.

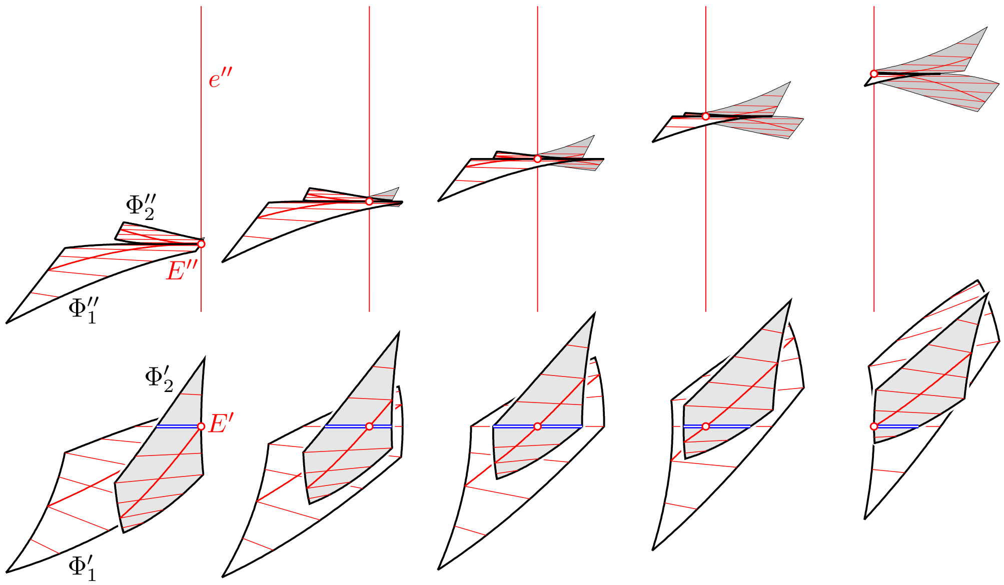

Figure 9: Different postures of Φ_1 and Φ_2 with *line contact* (double line) seen in direction of the contact normal e (top view — below) and in the front view (parallel e — above).

Corollary 2.4 *If two helical involutes Φ_1, Φ_2 are placed such that they are in contact along a common generator and if their axis are kept fixed, then Φ_1 and Φ_2 serve as gear flanks for a spatial gearing with permanent straight line contact.*
All contact normals are located in a fixed plane parallel to the two axes p_{10}, p_{20}.[3]

In Figs. 8–10 this gearing is illustrated: Fig. 8 shows a front view for an image plane parallel to p_{10}, p_{20} and e. Under the rotation about p_{10} the tooth flank Φ_1 is in contact along a straight line with the conjugate Φ_2 rotating about p_{20}. The flanks are bounded by two slip tracks and by two involutes, which are the intersections with planes perpendicular to the axes p_{10} or p_{20}, respectively. Five different positions of the flanks in mutual contact are picked out.

These five positions are also displayed one by one in Fig. 9 ($\theta = 0$) and in Fig. 10 ($\theta \neq 0$): The contact normal e of E is now in vertical position; the top view shows the orthogonal projection of Φ_1 and Φ_2 into the common tangent plane ε. Beside some generators of the tooth flanks also the slip tracks of a central point E are displayed.

The double line in the top view of Fig. 9 indicates the line of contact. Fig. 10 shows a case with point contact at E and the constant angle $\theta \neq 0$.

References

[1] Husty, M., Karger, A., Sachs, H., Steinhilper, W.: *Kinematik und Robotik*, Springer-Verlag, Berlin-Heidelberg 1997.

[3] This includes as a special case the line contact between helical spur gear as displayed in Fig. 1a.

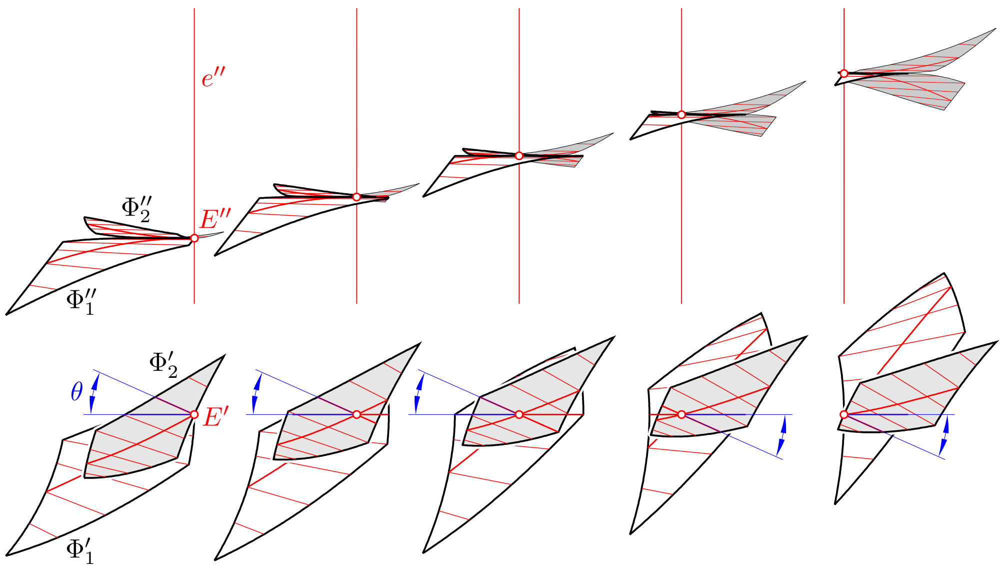

Figure 10: Different postures of Φ_1 and Φ_2 with *point contact* at E. The angle θ between the generators at E remains constant (Theorem 2.3).

[2] Phillips, J.: *General Spatial Involute Gearing*, Springer Verlag, New York 2003.

[3] Pottmann, H., Wallner, J.: *Computational Line Geometry*, Springer Verlag, Berlin, Heidelberg 2001.

[4] Stachel, H.: Instantaneous spatial kinematics and the invariants of the axodes. *Proc. Ball 2000 Symposium*, Cambridge 2000, no. 23.

[5] Wunderlich, W.: *Ebene Kinematik*, Bibliographisches Institut, Mannheim 1970.

Postal addresses

Hellmuth Stachel
Institute of Discrete Mathematics and Geometry
Vienna University of Technology
Wiedner Hauptstr. 8-10/104, A 1040 Wien
Austria